

# Travelling wave coil with limited SAR

M. Mueller<sup>1</sup>, S. Alt<sup>1</sup>, R. Umatham<sup>1</sup>, W. Semmler<sup>1</sup>, and M. Bock<sup>1</sup>

<sup>1</sup>Medical Physics in Radiology, German Cancer Research Center (DKFZ), Heidelberg, Germany

## Introduction

Travelling wave MRI [1] exposes the human body to high levels of SAR. Recently, a targeted travelling wave approach using an interrupted coaxial waveguide was presented [2,3] (Fig. 1) to constrict the SAR to a desired imaging region (IReg). The RF waves are guided to the IReg via a coaxial arrangement and are coupled into the patient at the gap between the inner conductor parts. With a variable IR an optimal SAR constriction can be achieved. In this work we

evaluate the performance of a coaxial system with different IRegs at 7 Tesla.

## Materials and Methods

All imaging experiments were carried out at a 7 T whole-body MRI system (Siemens Magnetom, Erlangen, Germany). A coaxial coil prototype of 30 cm outer diameter was connected to the MR system via a home-built TxRx switch. A cylindrical acrylic glass phantom (length: 80cm, diameter: 18cm) was placed in the center of the coaxial structure (Fig. 1). The phantom was filled with tissue-equivalent solution for 300MHz according to European standard EN 50361 (55,8% saccharose sugar, 37,2% de-ionized water, 5,9% sodium chloride, 1% hydroxyethyl cellulose and 0,1% bactericide (Preventol D7, Lanxess, Leverkusen/Germany)). Dielectric parameters and conductivity at 300 MHz were verified with the 85070E Dielectric ProbeKit (Agilent, Santa Clara, CA/USA). The width of the IReg was varied (5, 10, 15, 20 to 25cm). At each width the matching networks were adjusted.

Images were acquired with a 2D FLASH sequence (TE: 1.9ms, TR: 90ms, bandwidth: 610Hz/px, base resolution: 128, slice thickness: 20mm, excitation amplitude: 238.5 V, reference amplitude: 350V, averages: 8). Flip angle maps were measured by a pre-saturation based flip angle mapping sequence (Siemens, works-in-progress-version) with a rectangular pre-saturation pulse of 2ms, 100V and subsequent TFL readout (TE: 1.78ms, slice thickness: 20mm, matrix size: 64x64 FoV: 200x200mm) and long TR = 4000 ms to ensure complete longitudinal relaxation (measured T1: 465 ms). For evaluation, transversal slices were acquired and averaged within concentric rings of radii 5.3 cm and 6.4 cm around the phantom axis.

## Results and Discussion

The reflection parameters S11 and S22 inside the scanner at each gap size and were lower than -35 dB. The S21 values at the different gap sizes 5,10,15,20 and 25 cm were -6.0, 6.8, -8.8, -11.0 and -25.0 dB, respectively. The RF focuses to the different IRegs (Fig. 5), but also penetrates the lateral areas of the phantom. The highest signal intensity was seen at the phantom edges in the IReg. The illuminated area increases with the gap size.

With increasing gap size the maximum flip angle and signal intensity (Figs 2 and 3a) moves to the termination side of the travelling wave arrangement, and the maximum signal intensity decreases (Fig. 3a). The flip angle in longitudinal direction becomes more homogeneous, but decays less rapidly outside the IReg. In radial direction the flip angle increases with radius (Fig.3b). The full width at half width (FWHM) of the longitudinal flip angle distribution was calculated for gap sizes of 5, 10, 15, 20 and 25 to 9.3, 15.2, 17.9, 20.7 and 25.9cm, respectively (Fig. 5).

## Conclusion

The RF energy is focused to the imaging area, but is not fully restricted to it. The imaging region linearly increases with gap size for coaxial travelling wave coil arrangements. Still, the flip angle distribution shows a fast drop outside the IReg up to a gap size of 20cm. We can assume that the applied SAR will show an equivalent distribution and is therefore mainly contained within the IReg.

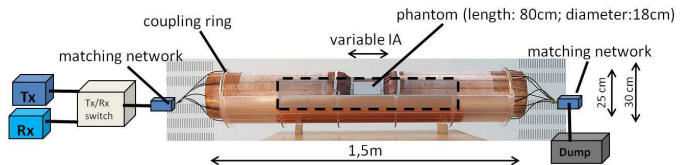


Fig. 1: Targeted travelling wave coaxial coil in a TX/RX setup; the phantom endings are located inside the inner conductors

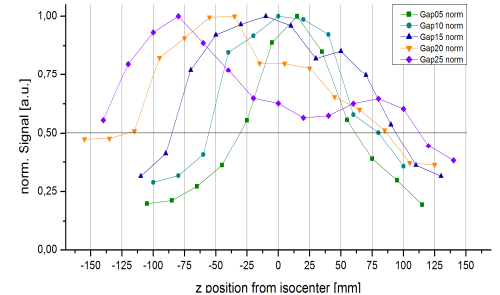


Fig. 2: Longitudinal signal distribution of different gap sizes, averaged over transversal slices and normalized to the maximum value of the respective distribution

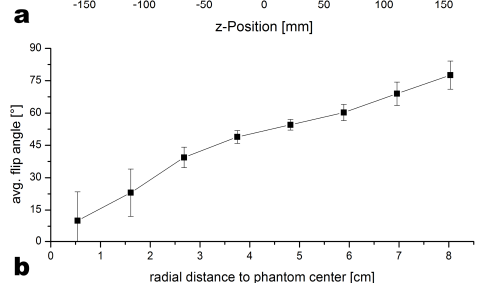
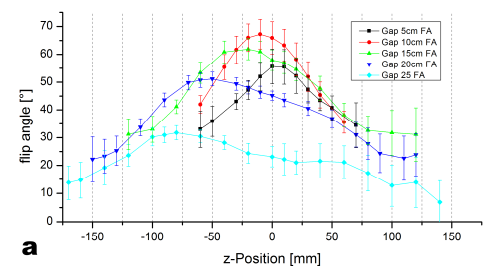


Fig. 3: a) longitudinal flip angle distribution averaged over a concentric ring in the transversal flip angle maps. Standard deviations are shown as error estimates.

b) radial distribution within the central transversal slice

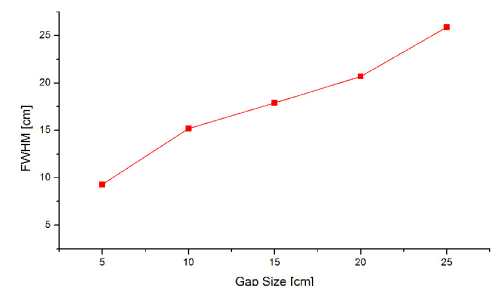


Fig. 4 FWHM in relation to the gap size

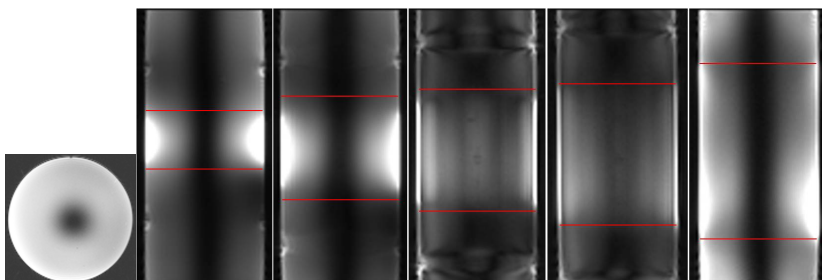


Fig. 5: Transverse (left) and coronal FLASH image through the phantom iso-center at different gap sizes (5, 10, 15, 20 and 25cm). The red lines indicate the size of the FWHM.

[1] Brunner et al, Nature 2009 457(7232)

[2] Mueller M.et al; Proc. Intl. Soc. Mag. Reson. Med. 18 (2010): 2580

[3] Alt S et al, Proc. Intl. Soc. Mag. Reson. Med 18:3559 (2010)